A Novel Thick-Film Piezoelectric Slip Sensor for a Prosthetic Hand

Darryl P. J. Cotton, *Student Member, IEEE*, Paul H. Chappell, *Member, IEEE*, Andy Cranny, Neil M. White, *Senior Member, IEEE*, and Steve P. Beeby, *Member, IEEE*

***Abstract*—The ability to mimic the tactile feedback exhibited by the human hand in an artificial limb is considered advantageous in the automatic control of new multifunctional prosthetic hands. The role of a slip sensor in this tactile feedback is to detect object slip and thus provide information to a controller, which automatically adjusts the grip force applied to a held object to prevent it from falling. This system reduces the cognitive load experienced by the user by not having to visually assess the stability of an object, as well as giving them the confidence not to apply unnecessarily excessive grip forces. A candidate for such a sensor is a thick-film piezoelectric sensor.**

The method of fabricating a thick-film piezoelectric slip sensor on a prototype fingertip is described. The construction of experimental apparatus to mimic slip has been designed and analyzed to allow the coefficient of friction between the fingertip and the material in contact with the fingertip to be calculated. Finally, results show that for a coefficient of friction between the fingertip and grade P100 sandpaper of approximately 0.3, an object velocity of 0.025 ± 0.008 ms^{-1} was reached before a slip signal from the piezoelectric sensor was able to be used to detect slip. It is anticipated that this limiting velocity will be lowered (improved) in the intended application where the sensor electronics will be powered from a battery, connections will be appropriately screened, and if necessary a filter employed. This will remove mains interference and reduce other extraneous noise sources with the consequence of an improved signal-to-noise ratio, allowing lower threshold values to be used in the detection software.

***Index Terms*—Piezoelectric thick-film, slip sensor, Southampton hand.**

I. Introduction

THE INCLUSION of a slip sensor in a prosthetic hand is thought to be advantageous in controlling both multiple degree-of-freedom (DOF) hands and conventional single DOF devices. A slip sensor would be used as part of a control system to automatically adjust the force applied to an object if it begins to slip from the hand. This would remove the need for the user to visually assess the object they are grasping, as well as reduce the need to apply large forces to the object. Many different slip sensor solutions have been investigated by a number of researchers with limited success. Although today there are still no real slip sensors included in any commercially available hand, the idea of including them into a design can be tracked back to the 1960s [1].

There are a range of applications throughout industry for slip detection devices, such as vehicle anti-lock braking systems (ABS), traction control, robotic grippers, and object handling (specifically with hazardous materials). Some of the existing solutions to these industrial problems include a magnetic roller ball sensor or rotating encoder [2]. However, the majority of these existing solutions are not suitable for inclusion in a prosthetic hand device due to the need for an anthropomorphic appearance, low weight, and low-power consumption.

Piezoelectric thick-film sensors are a prime candidate for a slip detection sensor. These sensors produce charge across their surfaces when mechanically deformed (for example, when acted upon by a force). This is known as the direct piezoelectric effect. They have a sensitivity of up to 130 pC/N [3] compared with a PVDF sensor of only 20–30 pC/N. The thick-film printing technique also allows sensors to be repeatedly and accurately placed directly onto the mechanical structure of a prosthetic hand at a low cost. In this case, a cantilever beam fingertip has been selected. Thick-film piezoelectric sensors have proved their ability to detect the vibrations caused by slip [4], [5]. However, the sensor's ability has not previously been quantified in terms of the initiation of object slip.

A. Methods of Slip Prevention

A review of the literature reveals several different designs for preventing object slip in a prosthetic hand: one of the most popular is the piezoelectric sensor. Most of the work done with this type of sensor has used polyvinylidene fluoride (PVDF) strips [6]–[8], most likely because they are cheap, easily available, and come ready to use. There are, however, a number of limitations with this type of sensor such as a low sensitivity of around 20–30 pC/N and a high sensitivity to temperature change [9]. The sensor activity changes by approximately 0.5% per °C, which in the operating temperature range of a prosthetic hand of −30 °C in cold conditions to 50 °C (or potentially higher) when holding a hot object means a 40% change in the activity of the sensor would occur.

Dario *et al.* [7] developed a fingertip for use on a robotic arm, using an overlapping configuration of eight rows and eight columns of piezoresistive silk-screened ink, to create an array of 64 force sensors. A piezoelectric ceramic bimorph element was also attached to the fingertip to be used as a dynamic force sensor in an attempt to detect slip. The piezoresistors had a measuring force range of 0.1–8 N with a maximum spatial resolution of 1 mm, which is the maximum resolution that a human fingertip can differentiate between two different objects

Manuscript received June 15, 2006; revised August 24, 2006 and October 13, 2006; accepted October 13, 2006. The associate editor coordinating the review of this paper and approving it for publication was Dr. Subhas Mukhopadhyay.

The authors are with the School of Electronics and Computer Science, University of Southampton, Southampton SO17 1BJ, U.K. (e-mail: dpjc03r@ecs.soton.ac.uk; phc@ecs.soton.ac.uk; awc@ecs.soton.ac.uk; nmw@ecs.soton.ac.uk; spb@ecs.soton.ac.uk).

Color versions of one or more of the figures in this paper are available online at http://ieeexplore.ieee.org.

Digital Object Identifier 10.1109/JSEN.2007.894912

[8]. The piezoresistors were successfully used to detect the grip or normal force on an object, as well as any movement of the object in the grip associated with slip. The piezoelectric dynamic force sensor was not characterized for its slip sensing capabilities in this paper.

Mingrino *et al.* [6] investigated a method to detect the incipient slip by monitoring the normal and shear force from a grasped object. The force sensor used comprised four piezoresistive thick-film force sensors printed on a polymer film in a square configuration with each sensor being printed in a triangular shape pointing towards the center of the square. The force applied by gripping an object is coupled to the center of the sensor configuration via a cylinder. This then allows the normal force and tangential force of the object to be calculated from the force ratios applied to each thick-film resistor. By monitoring the normal and tangential forces and keeping the normal to tangential force ratio above a predefined level sets the lowest coefficient of friction limit to that value. Below this value, determined by the properties of the prosthesis glove and object, slip will occur and conversely above that value no slip will occur. It is, therefore, advantageous to set a high safety factor, allowing a range of objects to be gripped. This is essentially the same method used in the OttoBock Sensor Hand™ Speed [10].

Cutkosky and Tremblay [8], [11] developed a slip sensor using accelerometers mounted on the inside of a silicone rubber skin. To allow the accelerometers to vibrate, a dome shaped piece of foam bulks out the skin producing a fingertip shape. The foam and the side of the rubber skin were both attached to a solid mounting base. The skin was made from a self-leveling silicon rubber 1.5 mm thick with small nibs on the outside surface. This is so that when slippage occurs some of the nibs at the edge of the grasped object break contact and snap back to their original position causing local vibrations. These vibrations were then picked up by the accelerometers and PVDF strips which were attached to the underside of the skin. The signals obtained from the accelerometer have been successfully used in conjunction with a tangential normal force sensor to control a five linkage robotic finger, limiting the slip of an object occurring even when a sudden change in load was applied.

B. The Southampton Hand

The Southampton Hand Project has been ongoing since its beginning in the 1960s investigating a range of potential improvements to prosthetic hands. These improvements include the control system, mechanical functionality, and the integration of sensors for automatic control. The current mechanical design of the hand is based on the Southampton REMEDI Hand [12], [13] and can be seen in Fig. 1. The hand consists of six small electrical motors, two of which are used to actuate the extension-flexion and rotation movements of the thumb with each of the remaining four motors being assigned to individual fingers. Each finger is made from six bar linkages which when extended or flexed curl in a fixed anthropomorphic trajectory [14]. To reduce the power used to hold an object, the fingers are driven via a worm wheel gear configuration, thus preventing the finger being back driven after power is removed from the motor. The worm wheel drive also increases the torque produced from the small motors to provide a 9 N grip force at the end of each finger.

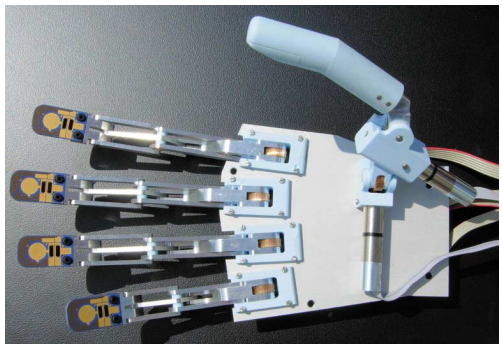

Fig. 1. The Southampton Hand.

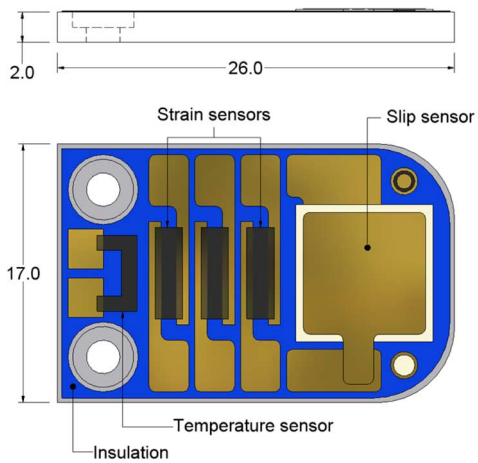

Fig. 2. Prototype fingertip (all dimensions in millimeters).

The hand is controlled using the Southampton adaptive manipulation scheme (SAMs) control system in conjunction with a three DOF myo-classifier developed at the University of New Brunswick [15]. This controller allows up to four different grip postures to be preprogrammed into the hand and uses information provided by sensors in the hand to control the force applied to an object by each of the fingers and the thumb. For example, if an object begins to slip from the hand, an increase in force will be applied until slip is no longer detected. Or if a high temperature is detected which may damage the prosthesis, the hand could alert the user to take appropriate action. This automatic control further removes the mental strain or concentration required to operate the hand.

Previous work has investigated the potential of optical and capacitive-based force sensors, with microphones to detect slip at the fingertips [16]–[18]. The work reported here represents an alternative method for producing these types of sensor.

II. Fingertip Design

Recent research at Southampton has concentrated on producing an array of sensors on a fingertip shaped beam. This has been accomplished using thick-film printing techniques [19]. Fig. 2 illustrates a prototype fingertip with three types of printed sensor. Each sensor replicates a type of sensor found in the natural human hand [20]. The piezoelectric dynamic force sensor is used to detect slip in a similar manner to the fast adapting mechanoreceptive afferent units. So for example, when a step

input is applied, a signal is generated which decays with time. The sensor is thus used to detect vibrations across the fingertip associated with slip.

The piezoresistive strain sensors act as slow adapting mechanoreceptive afferent units. The fingertip is modeled on a cantilever beam structure with the piezoresistors located close to the root where the maximum strain is produced [21]. When a force is applied to the end of the fingertip, the structure bends and the resistance of the piezoresistors change in proportion to the applied force and the output remains at a constant value until the force changes. The piezoresistors are also arranged in such a manner as to allow an accurate force to be calculated independently of the position of the load (as long as the force is applied distal to the resistors location on the beam) using resistance ratios. This technique and experimental results are described in more detail in [5] along with the characteristics of the force and temperature sensors.

The temperature sensor (formed from a thermistor paste) represents the thermosensitive units found in the human hand and can be used for temperature compensation of the other sensors, which could range from -30 °C in cold climates to over 50 °C when holding hot objects. The temperature sensor can also be used to detect if an object gripped by the hand is too hot or too cold, and thus prevent damage to the prosthesis by automatically releasing the object.

A. Sensor Fabrication

Fingertip shapes were cut from a 2-mm-thick stainless steel (type 430S17) plate, then degreased using acetone and subsequently rinsed in deionized water to remove any potential contaminants which could affect the print quality. To isolate the sensors electrically from the stainless steel substrate three layers of dielectric paste (ESL 4986) were successively printed, left for 10 min to level out before being dried using an IR heater for 10 min at approximately 150 °C, and then fired in a belt furnace for approximately 60 min, reaching a peak temperature of 850 °C. A single layer of gold paste (ESL 8836) was then printed on top of the dielectric, left to level, dried and fired (using the same parameters used to create the dielectric layer) to form the bottom electrodes for each of the sensors. The piezoresistors (ESL 3914) and thermistor (ESL PTC-2611) were subsequently printed and fired in a further two stages using the same parameters. The PZT paste composition used in this application was developed at the University of Southampton. The paste comprises a mixture of two different sized PZT-5H powder grains of 2 μm (72% total weight) and 1 μm (18% total weight) in a 4:1 mixture weight ratio, mixed with 10% by total weight powdered glass binder (CF7575) and a solvent (ESL 400) to make it screen printable. Details of the paste preparation and optimized processing parameters can be found in [22]. The piezoelectric layer was printed and left to level for approximately 10 min before being dried in an IR drier at 150 °C. A second layer was then printed on top of the first, left to level for 10 min before again being dried at 150 °C in an IR drier. The two layers were then co-fired at a peak temperature of 950 °C, producing a film thickness of approximately 100 μm. Finally, a top gold electrode (ESL 8836) was printed, left to level, dried and fired using the same parameters used to define the gold bottom electrodes. Fig. 3 illustrates the printed layers on the fingertip.

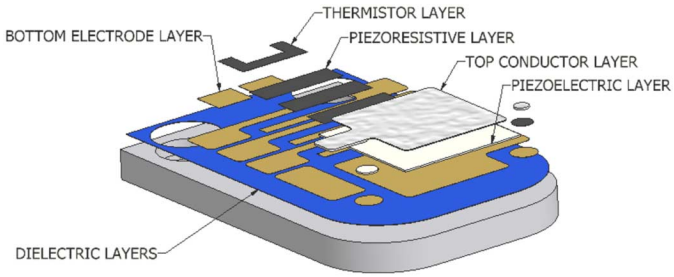

Fig. 3. Printing layers required to create prototype fingertip.

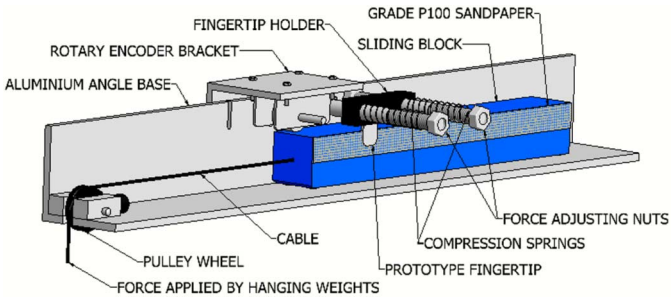

Fig. 4. Slip test apparatus.

To activate the piezoelectric sensor a poling process was used, whereby a poling field of 4 MVm^{-1} (approximately 400 V) was applied across the piezoelectric layer for 30 min at 150 °C. The sample was then allowed to cool to room temperature before the voltage was removed. The d_{33} (sensitivity of the samples) was measured using a take control PM35 piezometer [23] and revealed a sensitivity value of around 46 ± 2 pC/N.

B. Experimental Setup

In order to quantify the ability of the piezoelectric sensor to detect slip, it must be compared in some way to the real slip of an object. To achieve this, a slip apparatus was designed and built. It incorporated a rotary encoder to monitor object movement and acceleration, thus allowing a comprehensive comparison of the object's movement with that of the slip sensor signal.

Fig. 4 illustrates the slip test equipment used throughout the experiments. The test equipment comprises a sliding block made from aluminium with four nylon headed screws attached to the bottom and two nylon screws attached to the side of the block. These screws allow the block to slide more freely against the side and the bottom of the aluminium angle base.

The fingertip is bolted to a plastic block held up by two studs in the same manner as it would be connected to the end of a prosthetic finger. To allow different forces to be applied to the fingertip two compression springs were placed over the studs so that when the nuts are tightened the springs apply a force to the block, which is then coupled through the end of the fingertip and onto the sliding block. This feature allows a range of applied fingertip forces to be analyzed.

To replicate slip, weights are attached to the front of the aluminium block via a metal cable and hung over a pulley attached to the base. When the weight is released it drops to the floor causing the "sliding block" to slip past the fingertip.

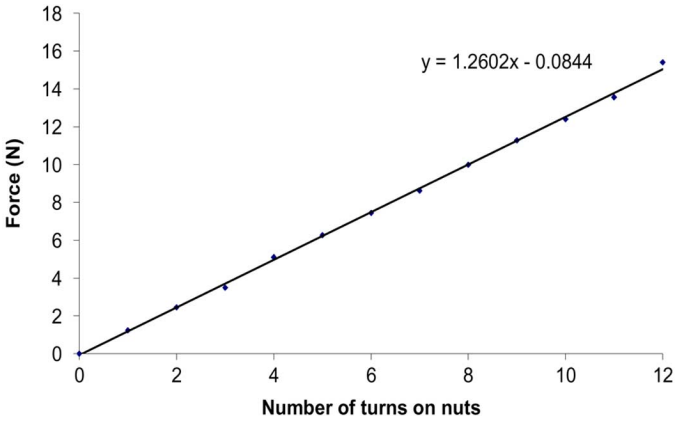

Fig. 5. Force calibration of springs.

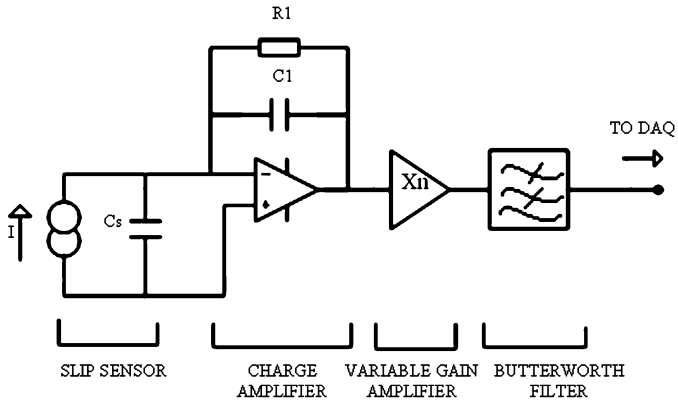

Fig. 6. Charge amplifier with gain control and eight-pole Butterworth filter.

A HEDS-5540 three channel rotary encoder with a resolution of 500 pulses per revolution (ppr) was mechanically coupled to the top of the block via a wheel using the bracket shown in Fig. 4. The wheel has a 44 mm diameter and a circumference of approximately 138 mm. With 500 ppr from the encoder, a linear resolution of 0.276 mm per pulse is obtained.

C. Calibration of Applied Force

In order to calibrate the force applied by the fingertip, a Mecmesin Compact Gauge [24] force measuring device was used to measure the force at the fingertip holder block whilst the nuts were tightened together one full turn at a time. The Compact Gauge force measuring device is a handheld force gauge with a digital readout capable of measuring compression and tension forces up to 50 N with a resolution of 0.25 N. Fig. 5 shows that the springs obey Hooke's law

$$\mathrm{F} = \mathrm{kx} \tag{1}$$

where F is the force on the spring, k is the spring constant, and x is the change in length of the spring, and that for a full turn on both bolts the fingertip force increased by approximately 1.26 N.

D. Data Collection

In order to easily manipulate and analyze the signals, data was collected using a National Instruments 6036E data acquisition card (DAQ) and a purpose built program written in LabVIEW™ 7.1. The 6036E is a 16-bit card with 16 analogue inputs, 2 analogue outputs, and a maximum sampling rate of 200 kS/s. The slip sensor and encoder signals were sampled at a rate of 10 kS/s throughout each trial to allow all signals up to 5 kHz to be accurately represented in a digital form [25].

E. Electrical Circuit Design

The charge output from all piezoelectric materials is generally very low and traditionally measured in pC/N. This signal has to be converted to a voltage and amplified so it can be accurately recorded. Fig. 6 illustrates the process used to amplify and filter the signal before the data was recorded. Initially, the charge from the sensor was converted into a voltage and amplified using a charge amplifier. The charge amplifier is built around the MXL1007 operational amplifier. The capacitances of the piezoelectric sensors differ between samples due to slight variations in sample thickness and are typically in the range of 1–7 nF $(\mathrm{C_s})$. The gain of the charge amplifier was kept as near to unity as possible by selecting a feedback capacitor with a similar value $(\mathrm{C_1})$. A second amplifier provides further gain. To avoid aliasing issues an anti-aliasing filter was incorporated into the circuit to allow frequencies above 1/2 of the sampling rate to be rejected, thus allowing an accurate digital picture of the signal to be generated. For this purpose, a Maxim 291 switched capacitor low-pass eight-pole Butterworth filter was selected.

The value of the feedback resistor R1 in the initial stage of the charge amplifier is very important since it controls the decay time and amplitude of the output from the piezoelectric sensor. A high-value resistor will produce a longer decay time with a high signal output, while a small value resistor will produce a faster decay time with a low signal output. For this particular application, a 1 M Ω resistor was found to produce an optimal response.

F. Analysis of the Forces Acting on the Slip Test Apparatus

Analyzing the forces acting upon the test rig components and performing some simple experiments allowed the coefficient of friction between the fingertip and the sandpaper adhered to the sliding block to be calculated. Using similar methods, the coefficient of friction between the test rig base and the nylon screws was also obtained. The coefficient of friction between the fingertip and contacting surface is important to enable a comprehensive evaluation of the sensor's capabilities when detecting slip on everyday objects as there is expected to be a limit at which the coefficient of friction is too low to produce a signal. This limit is not expected to affect the use of the sensor as the user may be able to visually assess an object before deciding upon the grasp pattern they will use to pick up or hold that object. For example, most people would cup an ice cube in the palm of their hand while holding it rather than use their fingers and thumb.

The slip test apparatus has been modeled in Fig. 7 with all of the forces acting upon the test rig during its operation denoted. For ease of analysis, Fig. 7 has been divided into smaller free body diagrams (FBD) shown in Figs. 8–10, where the following notation is used:

$\mathrm{A_1}$ is the linear acceleration of the "sliding block" (m $\mathrm{s^{-2}}$);
$\mathrm{A_2}$ is the linear acceleration of the "falling mass" (m $\mathrm{s^{-2}}$);

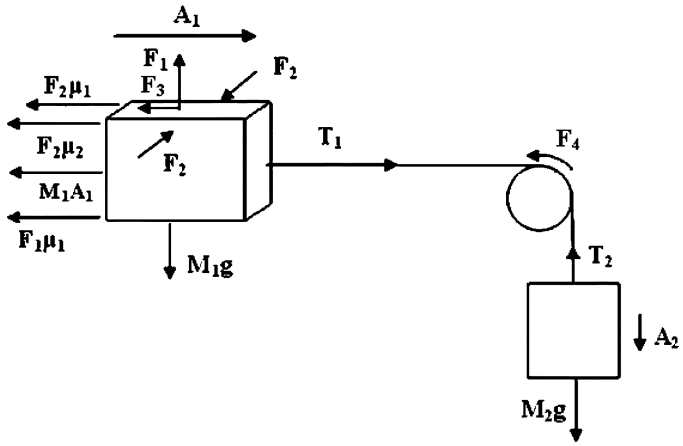

Fig. 7. Test rig system with forces and accelerations labeled during normal operation.

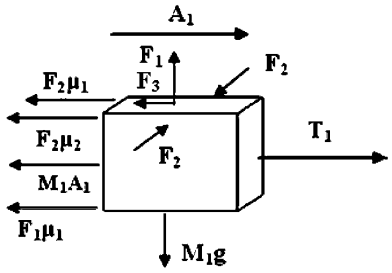

Fig. 8. Free body diagram of sliding block.

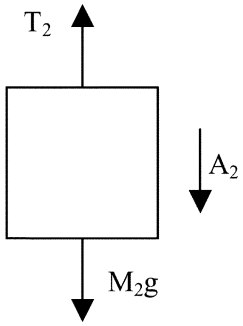

Fig. 9. Free body diagram of falling mass.

F_1 is the normal force produced by the mass of the block (N);
F_2 is the force applied by the fingertip (N);
F_3 is the inertial and frictional forces from the encoder (N);
F_4 is the inertial and frictional forces from the pulley (N);
M_1 is the mass of the "sliding block" (kg);
M_2 is the mass of the "falling mass" (kg);
T_1 and T_2 are the tension forces in the cable (N);
μ_1 is the coefficient of friction between the nylon screws and the aluminium base;
μ_2 is the coefficient of friction between the fingertip and the material adhered to the sliding block.

I) Analysis of the Sliding Block:
Resolving forces horizontally

$$\mathrm{T}_1 - \mathrm{M}_1\mathrm{A}_1 - \mathrm{F}_3 - \mathrm{F}_1\mu_1 - \mathrm{F}_2\mu_2 - \mathrm{F}_2\mu_1 = 0. \quad (2)$$

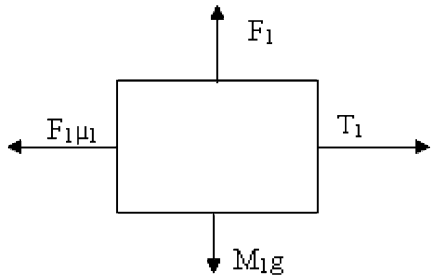

Fig. 10. Free body diagram of sliding block being pulled along at a constant velocity.

The tension force in the metal cable T_1 is opposed by the friction forces created between the nylon screws on the sliding block and the bottom $(\mathrm{F}_1\mu_1)$ and side $(\mathrm{F}_2\mu_1)$ of the aluminium base. Friction forces created between the fingertip and material adhered to the sliding block $(\mathrm{F}_2\mu_2)$, as well as inertia forces from the sliding block itself $(\mathrm{M}_1\mathrm{A}_1)$ and the inertia and fictional forces from driving the motor encoder (F_3) also oppose the tension force in the metal cable.
Resolving forces vertically

$$\mathrm{F}_1 - \mathrm{M}_1\mathrm{g} = 0. \quad (3)$$

II) Analysis of the Falling Mass: There are no forces acting in the horizontal plane, therefore resolving forces vertically

$$\mathrm{T}_2 - \mathrm{M}_2\mathrm{g} - \mathrm{M}_2\mathrm{A}_2 = 0. \quad (4)$$

Assuming negligible inertia and negligible frictional losses of the pulley and encoder assembly and that the coupling wire is inextensible provides the following linking equations:

$$\mathrm{F}_3 = 0 \quad (5)$$
$$\mathrm{F}_4 = 0 \quad (6)$$
$$\mathrm{T}_1 = \mathrm{T}_2 \quad (7)$$
$$\mathrm{A}_1 = \mathrm{A}_2. \quad (8)$$

Substituting (3) to (8) into (2) yields the expression

$$\mathrm{A}_1[\mathrm{M}_1 - \mathrm{M}_2] + \mu_1[\mathrm{F}_2 + \mathrm{F}_1] + \mu_2\mathrm{F}_2 - \mathrm{M}_2\mathrm{g} = 0. \quad (9)$$

This expression leaves three unknowns μ_1, μ_2, and A_1, which can all be found experimentally.

III) Experimentally Determining μ_1: To determine the sliding coefficient of friction μ_1, the sliding block was pulled along the base of the test rig at an approximate constant velocity by hanging weights on the metal cable, suspended over the pulley, and without the fingertip in contact with the block. The force T_1 was then calculated from the weight required to make the block slide (cf. Fig. 10).
Resolving forces horizontally

$$\mathrm{T}_1 - \mathrm{F}_1\mu_1 = 0. \quad (10)$$

The experiment was conducted six times and an average T_1 value of approximately 2.7 N was recorded (cf. Table I). The

TABLE I
AVERAGE COEFFICIENT OF FRICTION VALUES RECORDED AT DIFFERENT APPLIED FORCES

F_2 Value (N)	Average T_1 Value (N)	Average μ_2 Value
0	2.70 ± 0.00	N/A
1	3.15 ± 0.05	0.27 ± 0.05
2	3.65 ± 0.05	0.29 ± 0.03
3	4.20 ± 0.00	0.31 ± 0.00
4	4.75 ± 0.05	0.32 ± 0.01

mass of the sliding block M_1 was 1.336 kg and taking the acceleration due to gravity to be 9.81 ms^{-2} allows the coefficient of friction between the nylon screws and aluminium test rig base to be calculated by substituting (3) into (10)

$$\mu_1 = \frac{T_1}{M_1 g} \approx 0.2. \tag{11}$$

The value determined for μ_1 of 0.2 is comparable with that found in the literature, giving confidence in this experimental method. For example, Carvill quotes the coefficient of friction for Nylon on steel under low pressure and with no lubrication as lying within the range 0.3 to 0.5 [21].

IV) Experimentally Determining μ_2: The same procedure was then applied to the test rig to calculate the sliding coefficient of friction between the fingertip and the grade P100 sandpaper adhered to the sliding block (μ_2), with a known force (F_2) applied to the sliding block by the fingertip (cf. Fig. 8). Resolving forces horizontally

$$T_1 - F_2\mu_1 - F_2\mu_2 - F_1\mu_1 = 0. \tag{12}$$

Rearranging (12) allows μ_2 to be calculated

$$\mu_2 = \frac{T_1 - F_1\mu_1}{F_2} - \mu_1. \tag{13}$$

In order to determine the coefficient of friction value, the force applied by the finger tip was increased from 0 to 4 N in 1 N increments. At each force increment, three T_1 force values were taken using the hanging weight method described earlier. The fingertip force was then reset and the experiment was repeated. The average of six runs was used to calculate an average μ_2 value at each force. These average values were then used to calculate an overall average μ_2 value of approximately 0.3. This compares favorably with published values of friction coefficients between similar types of materials (e.g., 0.2 for metal on metal, 0.4 for leather on metal and 0.5 for acrylic on metal) [21].

III. DATA COLLECTION AND ANALYSIS

The compression springs on the slip test apparatus were adjusted so that the fingertip applied approximately 1.25 N of force to a sheet of grade P100 sandpaper (with a similar surface roughness to that found on the striking surface of a match box), adhered to the side of the "sliding block" with double sided tape. A small stainless steel washer was glued to the back of the fingertip to prevent it being damaged by the sandpaper; this then couples any vibration forces to the sensor. Supported weights were attached to the cable connected to the "sliding block" (cf. Fig. 4). When released, this caused the block to accelerate past the fingertip, simulating slip. This experiment was subsequently repeated a number of times and the results analyzed in terms of the acceleration and velocity at which an initial slip signal was detected.

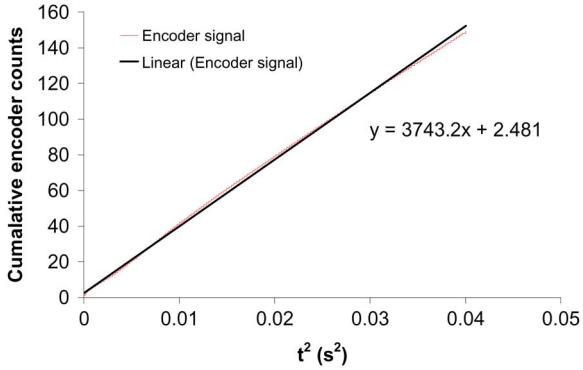

Fig. 11. Integrated encoder signal.

A. "Sliding Block" Acceleration

Calculating the acceleration and velocity of the "sliding block" allowed a direct comparison to be made between trials when the conditions of slip were the same and when they were not, and if this had any affect on the output signal. To obtain the acceleration of the block the cumulative encoder count was plotted with respect to the square of the time, as shown in Fig. 11. The value of the acceleration can then be determined by multiplying the gradient of the graph by twice the encoder resolution (from $s = ut + 1/2\,at^2$). Fig. 11 shows the encoder response to be linear indicating that the block is accelerating at a constant rate as expected. Similar responses were obtained for each of the trials, showing constant acceleration of the block in each case.

B. Setting a Threshold Level to Detect Slip Signal

A background noise reading was measured and rectified while the block was stationary. This revealed a peak noise level of 60 mV, allowing a suitable threshold of 100 mV to be selected for validating when the PZT signal was considered to be active. For each trial, the PZT and encoder signals were recorded simultaneously. The recorded PZT sensor signals were postprocessed in software. This involved first converting the digitized bipolar signals into their unipolar equivalents, in effect performing simple rectification. The resultant data set was then scanned in chronological order with each component of the data set being compared with the preset threshold level. Whenever the former exceed the latter, a threshold crossing event was recorded.

IV. RESULTS

Fig. 12 shows a typical signal obtained from the encoder and piezoelectric sensor when the block slides across the aluminium base with approximately 1.25 N of force being applied

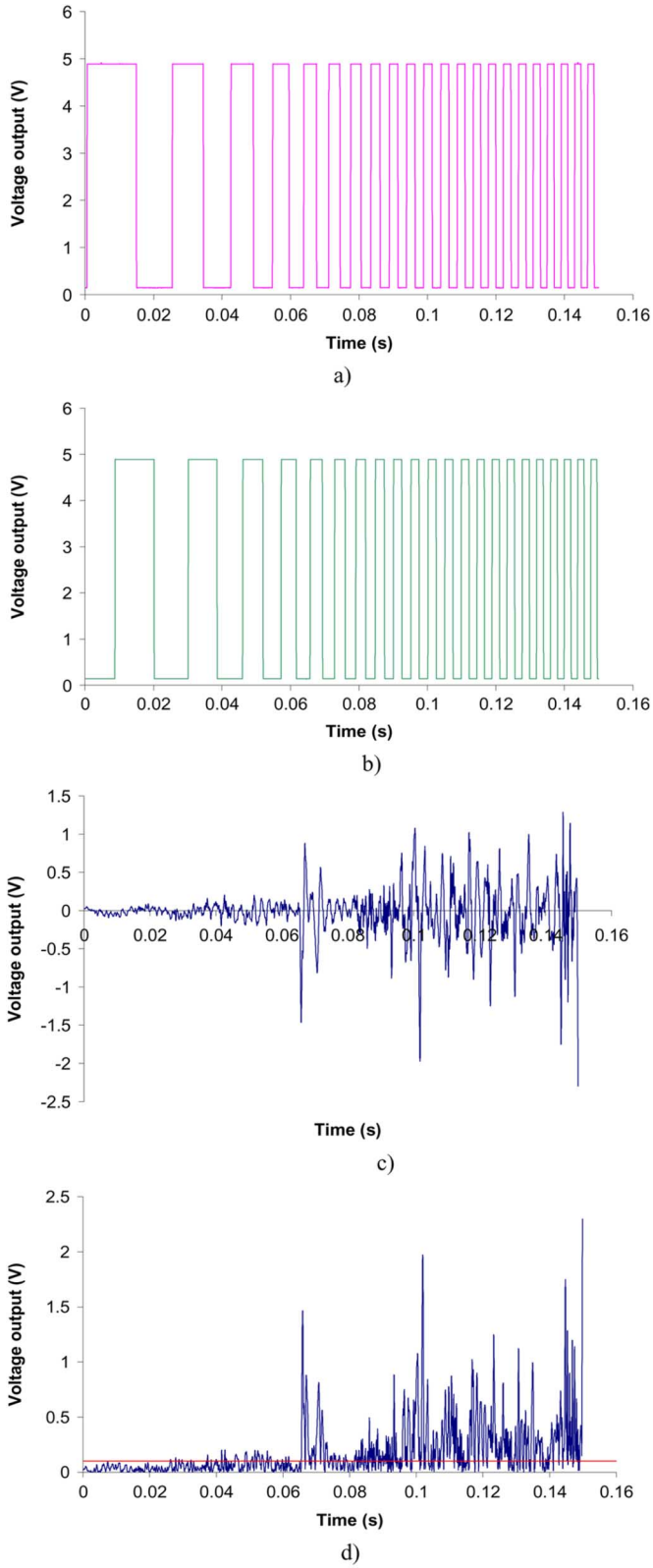

Fig. 12. Encoder and PZT signals before and after rectification. (a) Encoder signal 1 from sliding block. (b) Encoder signal 2 from sliding block. (c) Slip signal from PZT sensor. (d) Rectified slip signal from PZT sensor with superimposed 0.1 V threshold.

to the block by the fingertip. The encoder signals shown in Fig. 12(a) and (b) are 90° out of phase and both show a narrowing in pulse width with time. This indicates that the block is accelerating. Fig. 12(c) illustrates the output from the piezoelectric sensor. It is interesting to note that the amplitude of the sensor signal tends to increase as the block accelerates. Finally, Fig. 12(d) shows the rectified piezoelectric sensors output with a superimposed threshold level of 100 mV.

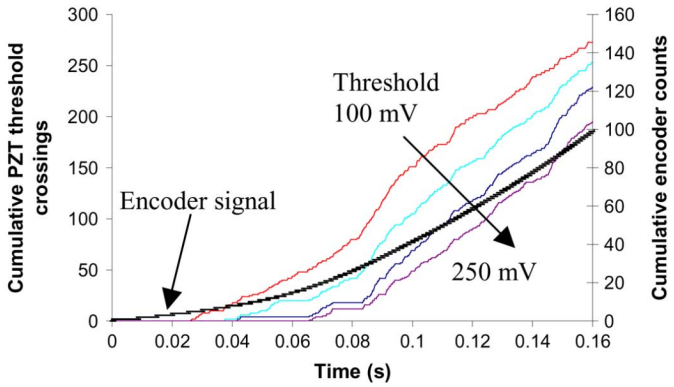

Fig. 13. Comparison of encoder signal to PZT slip signal for different threshold values ranging from 100 to 250 mV in 50 mV intervals.

Fig. 13 shows the cumulative number of postprocessed threshold crossing events, for different threshold levels, from a single PZT sensor when a fingertip force of 1.25 N was applied to the block. The encoder signal recorded during the acquisition of the sensor data is also shown in the figure. Since the encoder has a fixed resolution (1 count is 0.276 mm), then the sum of the encoder counts is a direct measure of the distance traveled by the "sliding block." The encoder and PZT sensor signals are sampled at a fixed rate, therefore the gradient of the encoder signal represents velocity. It can be seen from the Fig. 13 that the gradient of the encoder signal increases over the duration of the experiment which implies that the velocity increases with time (left to right across the graph), i.e., the block is accelerating. This is confirmed in Fig. 12(a) and (b), where the period of the encoder signals is shown to decrease over the duration of the experiment. The processed PZT signal for each threshold level bisects the x axis at different times, and hence at different velocities. Fig. 12(d) shows that at higher threshold levels, threshold crossing events are not recorded until later on in the experiment (i.e., at higher velocities). Conversely, at lower threshold values, threshold crossing events are observed much earlier in the experiment when the PZT sensor exhibits larger magnitude signals (i.e., at lower velocities). Thus, there is a limiting velocity before which slip cannot be detected, and the value of this velocity is proportional to the magnitude of the threshold used when counting threshold crossing events. Ideally, slip should be detected at the lowest velocity possible but this is where a tradeoff exists: setting a threshold level too low means that extraneous noise could register as a threshold crossing event giving the impression that slip had occurred when it had not.

Fig. 14 shows the cumulative PZT sensor threshold crossing events recorded over the distance traveled by the sliding block (determined from the encoder count and encoder resolution) for four trials with a fingertip force of approximately 1.25 N on grade P100 sandpaper and with a sensor signal threshold value of 100 mV. The values of the linear regression coefficients (displayed in the legend) show the highly linear fit for each trial.

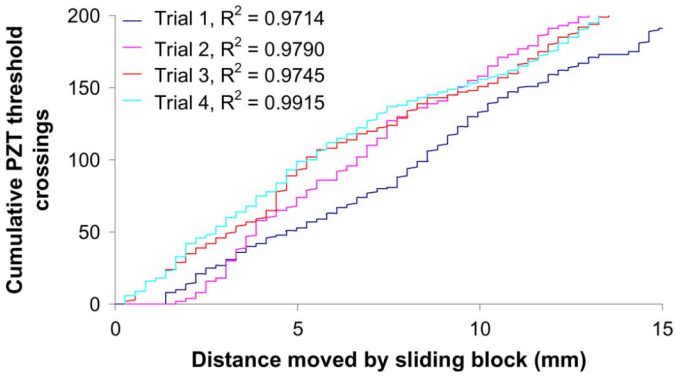

Fig. 14. Indication of sensor repeatability.

TABLE II
VELOCITY AND ACCELERATION AT WHICH SLIP WAS FIRST DETECTED

Trial	Velocity (ms^{-1})	Acceleration (ms^{-2})
1	0.0280	2.06
2	0.0334	1.55
3	0.0304	1.85
4	0.0176	1.44

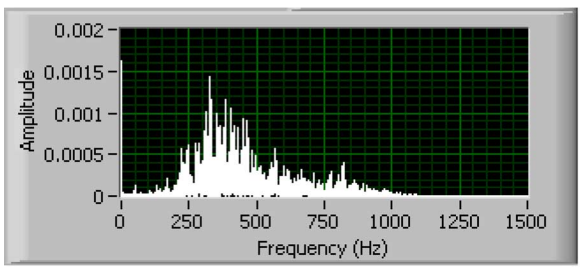

Fig. 15. Linear power spectrum FFT of trial 1.

At a threshold of 100 mV, slip was detected after the block had moved a distance between 1.10–1.66 mm. Table II shows that the velocity (determined from the encoder signals recorded simultaneously for each trial and from the sampling rate) at which the initial slip was detected was similar for the first three trials with an average value across all four trials of approximately 0.025 ± 0.008 ms^{-1}.

Fig. 15 shows a linear power spectrum FFT for a typical trial and reveals that the frequency content of the slip signal for this particular material combination is contained in the approximate range of 200–1000 Hz. This frequency range is likely to be dependant upon the type of material in contact with the fingertip and more tests on alternative materials are required before the application of filtering the sensor signal can be considered. However, if it is possible to filter out all of the lower frequencies up to around 150 Hz, then this would eliminate the mains noise (50 Hz) and allow a higher gain to be applied to the sensor output for improved signal to noise ratios. In the real application, noise will be reduced by locating the charge amplifier next to the sensor, which was not possible in this case due to the size of the prototype electronics—the signal being transferred through a 20 cm length of shielded cable. The circuit will also be powered by a battery which will also reduce noise levels. Fig. 16(a) and (b) show the output signal of the PZT sensor when it is lightly

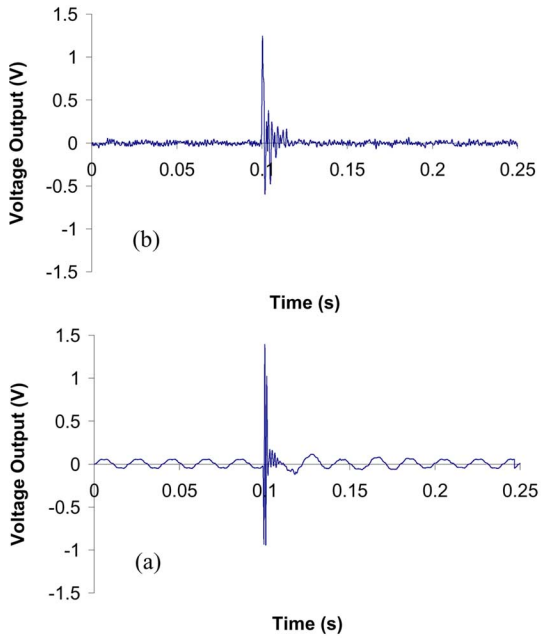

Fig. 16. Sensor output when the prototype fingertip is lightly tapped for (a) amplifier circuit powered from a mains source and (b) amplifier circuit powered from a battery source.

tapped. Fig. 16(a) shows the signal when the amplifier circuit is powered by a mains source, while Fig. 16(b) shows the output of the signal when the circuit is powered by a battery source. This reduced the peak noise level from 60 mV to approximately 30 mV. Both signals show a high initial output when tapped, which decays quickly with time and is notably different to that of the slip signal shown in Fig. 12. This characteristic could be utilized within a control system in the hand to avoid erroneous closure, for example, if the user accidentally bumps into an object or taps the table. The signal can also be used to indicate the first contact with an object when the hand is closing.

V. DISCUSSION

Fig. 12(c) shows evidence of a slip signal superimposed over background noise level (in this case, 50 Hz mains noise). However, the piezoelectric sensor's signal is much smaller than the noise signal and so a threshold cannot be accurately applied to it at an object velocity below 0.034 ms^{-1}. This suggests that if the 50 Hz noise is reduced by placing the electronics closer to the sensor and powering the electronics with a battery source, then the slip signal may be detectable at a lower velocity, and possibly before the object has moved 1 mm. The rejection of the 50 Hz noise would also allow a much higher amplifier gain to be applied, allowing the slip signals to be investigated in greater detail.

Fig. 14 shows an approximately linear relationship between the cumulative encoder counts and cumulative piezoelectric sensor's threshold crossing events. Since the encoder signal is a direct representation of the distance the object has moved, then it is reasonable to assume that the processed PZT signal also represents the distance moved by the object. The processed PZT signal, therefore, represents movement of the block, hence slip.

During everyday use there are a number of sources potentially producing erroneous signals from the slip sensor. These include bumping into an object or simply scratching your leg. For this reason, the sensor is intended to be used in conjunction with force sensors, motor encoders for finger tip position, and an intelligent control system. It is clear from comparing the piezoelectric sensor's response when lightly tapped to that of an object sliding that they are different and, hence, the tapping signals could be ignored. However, actions such as scratching your leg are likely to produce a similar response to a slip signal, so to avoid erroneous hand closure the position of the fingers and force applied to them can be taken into account, only allowing the signals from the slip sensor to be acted upon when the hand is in a grip mode.

It is likely that the surface properties (e.g., surface roughness, geometry, coefficient of friction between object and prosthesis) of a held object are related to the frequency and amplitude output of the piezoelectric sensor with respect to the velocity the object is traveling. If correct, then an FFT analysis maybe useful alongside other tactile information such as grip force in determining these characteristics. However, this type of analysis would still not be useful in controlling the force applied to an object within a prosthetics application. This is because a number of samples would have to be recorded before the surface properties could be determined. In real terms, this would mean the user of the prosthesis would have dropped the object they were holding before the surface properties and hence the force required to be applied to the object was determined. It is, however, a useful analysis in determining the frequencies which may be filtered out of the signal and also the minimum sampling rate which would be required in a prosthetics application to cover a range of surface geometries, coefficients of friction and velocities.

The analysis of the signal frequency content for different materials and surface geometries is important to enable an optimal frequency range to be selected for use in a prosthesis. This particular material combination shows very usable frequency content with no low frequencies, thus enabling mains noise to be removed and allowing enough characteristic data to be collected in a short period of time so that object slip can be detected quickly. The higher end of the frequency range is also not too high as to require a fast sampling device.

Other limitations will include low coefficients of friction not producing a large enough signal to define an object's slip, the damping effects of different glove types worn, and the position of the slip sensor in the prosthetic hand.

VI. Conclusion and Future Work

With a coefficient of friction of approximately 0.3 between the fingertip and sandpaper, a velocity of 0.025 ± 0.008 ms^{-1} was reached before a slip signal above the background noise was able to be used to detect slip. By reducing the threshold value used in the detection of threshold crossing events from 250 to 100 mV, it has been shown that the velocity at which the initial slip detection occurs is decreased. It is also evident that the slip signal from the PZT sensor began before it was detected at the threshold of 100 mV. Therefore, there is scope to reduce the background noise signal and use a much lower threshold value or increase the output gain, which would then allow the accurate detection of slip at lower velocities. This is the first experimental evidence that this type of thick-film piezoelectric sensor can be used to detect slip. The slip signal is a measure of relative velocity between the object and finger surface. It can be processed to obtain an estimate of the relative distance that an object has slipped.

This investigation has also proved the suitability of the apparatus to simulate slip under a range of conditions, e.g., acceleration, coefficient of friction, and fingertip force.

Further work is, therefore, required to investigate the lowest possible coefficient of friction required to trigger the signal at an acceptable object velocity with an optimal fingertip design.

References

[1] D. S. Childress, "Historical aspects of powered limb prosthesis," *Clinical Prosthetics and Orthotics*, vol. 9, pp. 2–13, 1985.

[2] H. R. Nicholls, *Advanced Tactile Sensing for Robotics*. Singapore: World Scientific, 1992.

[3] R. N. Torah, "Optimization of the Piezoelectric Properties of Thick-Film Piezoceramic Devices," Ph.D. dissertation, University of Southampton, Southampton, U.K., 2004.

[4] A. Cranny, D. P. J. Cotton, P. H. Chappell, S. P. Beeby, and N. M. White, "Thick-film force, slip and temperature sensors for a prosthetic hand," *Meas. Sci. Technol.*, vol. 16, pp. 1–11, 2005.

[5] A. Cranny, D. P. J. Cotton, P. H. Chappell, S. P. Beeby, and N. M. White, "Thick-film force and slip sensors for a prosthetic hand," *Sensors and Actuators A: Physical.*, vol. 123–124, pp. 162–171, 2005.

[6] A. Mingrino, A. Bucci, R. Mangni, and P. Dario, "Slippage control in hand prosthesis by sensing grasping forces and sliding motion," in *Proc. IEEE Int. Conf. Intell. Robots Syst., Advanced Robotic Syst. Real World (RSJ/GI)*, 1994, vol. 3, no. 3, pp. 1803–1819.

[7] P. Dario, R. Lazzarini, R. Magni, and S. R. Oh, "An integrated miniature fingertip sensor," in *Proc. IEEE 7th Int. Symp. Micromach. Human Sci.*, 1996, pp. 91–97.

[8] R. D. Howe and M. R. Cutkosky, "Sensing skin acceleration for slip and texture perception," in *Proc. IEEE Int. Conf. Robot. Autom.*, 1989, pp. 145–150.

[9] P. Ueberschlag, "PVDF piezoelectric polymer," *Sensor Rev.*, vol. 21, pp. 118–125, 2001.

[10] [Online]. Available: www.ottobock.co.uk. [Accessed on 3/4/06]

[11] M. R. Tremblay and M. R. Cutkosky, "Estimating friction using incipient slip sensing during a manipulation task," in *IEEE Int. Conf. Robot. Autom.*, 1993, vol. 1, pp. 429–434.

[12] C. M. Light, "An intelligent hand prosthesis and evaluation of pathological and prosthetic hand function," Ph.D. dissertation, University of Southampton, Southampton, U.K., 2000.

[13] C. M. Light and P. H. Chappell, "Development of a light weight and adaptable multiple axis hand prosthesis," *Med. Eng. Phys.*, vol. 22, pp. 679–684, 2000.

[14] G. Guo and W. A. Gruver, "Optimal design of a six bar linkage with 1 DOF for an anthropomorphic three jointed finger mechanism," in *Proc. Inst. Mech. Eng.*, 1993, vol. 207, pp. 185–190.

[15] C. M. Light, P. H. Chappell, B. Hudgins, and K. Engelhart, "Intelligent myoelectric control of hand prosthesis," *J. Med. Eng. Technol.*, vol. 26, no. 4, pp. 139–146, 2002.

[16] C. M. Light and P. H. Chappell, "Development of a light weight and adaptable multiple axis hand prosthesis," *Med. Eng. Phys.*, vol. 22, pp. 679–684, 2000.

[17] P. H. Chappell and J. A. Elliott, "Contact force sensor for artificial hands with a digital interface for a controller," *Measure. Sci. Technol.*, vol. 14, pp. 1275–1279, 2003.

[18] P. J. Kyberd and P. H. Chappell, "Characterization of an optical and acoustic touch sensor for autonomous manipulation," *Measure. Sci. Technol.*, vol. 3, no. 10, pp. 969–75, 1992.

[19] P. J. Holmes and R. G. Loasby, *Handbook of Thick-Film Technology*. Ayr, Scotland: Electrochemical Publications Limited, 1976.

[20] R. S. Johansson and A. B. Valbo, "Tactile sensory coding in the glabrous skin of the human hand," *Trends in Neurosciences*, vol. 6, pp. 27–32, 1983.

[21] J. Carvill, Mechanical Engineer's Data Handbook 2005, ISBN 0 7506 1960 0.

[22] R. Torah, S. P. Beeby, and N. M. White, "An improved thick-film piezoelectric material by powder blending and enhanced processing parameters," *IEEE Trans. Ultrasonics, Ferroelectrics, and Frequency Control*, vol. 52, no. 1, pp. 10–16, 2005.
[23] [Online]. Available: www.piezotest.co.uk/d33piezometer.html(Accessed on 23/08/06)
[24] [Online]. Available: www.mecmesin.com/ucm/home/product_view.asp?proID=101&range=39(Accessed on 23/08/06)
[25] S. W. Smith, *The Scientists and Engineer's Guide to Digital Signal Processing*, 2nd ed. San Diego, CA: Calif. Tech. Publishing, Electronic version, 1997–1999, ISBN 0-96601-6-8.

Darryl P. J. Cotton (S'05) received the B.Eng. (Hons) degree from the Department of Mechanical Engineering, Newcastle University, Newcastle, U.K., in 2003. He is currently working towards the Ph.D. degree at the School of Electronics and Computer Science, University of Southampton, Southampton, U.K., investigating the potential for integrating thick-film sensors into prosthetics.

He has a number of publications in the field of thick-film sensors.

Mr. Cotton is an associate member of the Institute of Mechanical Engineers.

Paul H. Chappell (M'05) graduated with a First-Class Honors degree in electronics from the University of Sussex, Brighton, U.K., and received the Ph.D. degree in control engineering from the University of Southampton, Southampton, U.K.

He is a Senior Lecturer in the Electronics Systems Design Research Group within the School of Electronics and Computer Science, Southampton University. He has also designed power electronic converters for industrial applications. He is an author of over 90 publications (journal papers, conference proceedings, chapters in books, and a patent). His research interests are in medical engineering, particularly prosthetics and functional electrical stimulation.

Dr. Chappell is a Chartered Engineer. He is a member of the Institution of Engineering and Technology and the Institute of Physics and Engineering in Medicine.

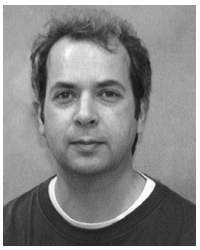

Andy Cranny graduated from the University of Coventry, Coventry, U.K., in 1985 with an Applied Physics degree (Hons), and received the Ph.D. degree from the University of Southampton, Southampton, U.K., in 1992, for a thesis on sensor array signal processing for cross-sensitivity compensation in nonspecific organic semiconductor gas sensors.

He is currently a Senior Research Fellow within the School of Electronics and Computer Science, University of Southampton. He has been employed at various times at the University, both in his present position and also within the School of Engineering Sciences, for over 15 years. He has also had industrial experience, working on fiber-optic preform analysis with GN NetTest for 15 months in the post of Senior Measurement Engineer and has held directorships with two technology orientated companies. He has a number of publications in the field of thick-film sensors for both physical and chemical parameters and is a coinventor on a number of patents.

Dr. Cranny is a member of the Institute of Physics and is a Chartered Physicist.

Neil M. White (M'02–SM'02) received the Ph.D. degree from the University of Southampton, Southampton, U.K., in 1988.

He holds a Personal Chair in the School of Electronics and Computer Science, University of Southampton He has been active in sensor development since 1985. He is Director and co-founder of the University of Southampton spin-out-company Perpetuum Ltd. He has considerable experience in the design and fabrication of a wide variety of sensors, formulation of novel thick-film sensing materials, and intelligent sensor systems. He has over 200 publications in the area of instrumentation and advanced sensor technology.

Prof. White is a Chartered Engineer, a Fellow of the IET, a Fellow of the IOP, and a Chartered Physicist.

Steve P. Beeby (M'03) received the B.Eng. (Hons) degree in mechanical engineering from the University of Portsmouth, Portsmouth, U.K., in 1992 and the Ph.D. degree from the University of Southampton, Southampton, U.K., in 1998.

His other research interests include energy harvesting for remote wireless sensor networks and he is the Project Coordinator of an EU funded STREP project entitled "Vibration Energy Scavenging (VIBES)." He is coauthor of *MEMS Mechanical Sensors* (Artech House). He has provided consultancy services to several companies. He is also interested in human biometric systems. He has over 120 publications in the field.

Dr. Beeby was awarded a prestigious EPSRC Advanced Research Fellowship in 2001 to continue his research into active thick-film materials development and their combination with micromachined devices. He is a member of the EPSRC Peer Review College, reviewer for numerous journal publications, a Chartered Engineer and Chartered Physicist.